Optics & Laser Technology 157 (2023) 108689

Contents lists available at ScienceDirect

Optics and Laser Technology

journal homepage: www.elsevier.com/locate/optlastec

Full length article

Cooling photoluminescent phosphors in laser-excited white lighting with three-dimensional boron nitride networks

Weixian Zhao [a,1], Bin Xie [b,1], Yang Peng [c], Song Xue [a], Xiaobing Luo [a], Run Hu [a,d,*]

[a] School of Energy and Power Engineering, Huazhong University of Science and Technology, Wuhan 430074, China
[b] School of Mechanical Science and Engineering, Huazhong University of Science and Technology, Wuhan 430074, China
[c] School of Ecological Construction and Environmental Protection, Jiangxi Environmental Engineering Vocational College, Ganzhou 341400, China
[d] Wuhan National Laboratory for Optoelectronics, Huazhong University of Science and Technology, Wuhan 430074, China

ARTICLE INFO

Keywords:
Laser diodes
Thermal quenching
Heat dissipation
Boron nitride
3D networks

ABSTRACT

Laser-excited white lighting, which is achieved by laser diodes and phosphor converters, has garnered increasing interest in recent years due to their high-power and high-brightness characteristics. Nevertheless, two long-standing thermal issues remain formidable: first, the photoluminescent phosphors also generate heat due to the Stokes loss, which are the second heat source in the packaging but long ignored; second, the phosphors are embedded in low-thermal-conductivity silicone and the generated heat is rather inefficient to dissipate. As a result, the accumulated heat leads to high temperature in phosphor particles and even thermal quenching, which deteriorate the luminescence, chromaticity, and reliability. In this work, these problems are successfully addressed by establishing three-dimensional (3D) boron nitride (BN) networks to cool the silicone-embedded phosphor particles in a facile and scalable method. When lighted under the driven current of 900 mA, the working temperature of phosphor layer is dramatically decreased by 95.2 °C with the 3D-BN network without sacrificing the luminescence and chromaticity. Such strategy with excellent cooling performance, high reliability, and easy scalability may hold great promise for broader optoelectronics applications beyond laser-excited white lighting.

1. Introduction

As the fourth generation of lighting source, light-emitting diodes (LEDs) have dominated the global lighting market in the last decade due to their advantages of high luminous efficiency, excellent color quality, and long lifetime [1–3]. However, the electro-optical conversion efficiency of LEDs suffers from a rapid decline with the increase of power density, thus limiting their further applications in high-power scenarios [4,5]. Alternatively, laser diodes (LDs), which can maintain high electro-optical conversion efficiency under high power density, have attracted extensive attention in recent years [6]. In addition, LDs also exhibit unique superiorities like low etendue, high optical energy density, and good monochromaticity, which make them expected to replace LEDs in high-power and high-brightness applications and become the next generation of solid-state lighting (SSL) source [7–9].

The most common way to achieve laser-excited white lighting is utilizing blue laser diode to excite yellow cerium-doped yttrium aluminum garnet (YAG:Ce) phosphors, in which case the yellow light excited from phosphors mixes with the transmitted blue light to form the white light [10]. However, there exist complex optical processes in the phosphor layer, including absorption, scattering and photoluminescence, which inevitably accompany with various losses, such as light absorption loss, quantum efficiency loss and Stokes loss [11,12]. These losses are eventually converted into heat, and the accumulation of heat will result in a sharp temperature increase of the phosphor layer. Previous studies have revealed that the luminescent efficiency of phosphor decreases with the rise of temperature, and a high temperature (>200 °C) even leads to silicone carbonization and phosphor thermal quenching [13,14]. Therefore, enhancing the heat transfer in phosphor layer is crucial for the long-term stability of laser-excited white lighting.

To tackle the thermal issue in the phosphor layer, many efforts have been devoted. For example, by resorting to high-temperature sintering or crystal growth technology, different kinds of phosphor composites were obtained to substitute the conventional phosphor colloid,

* Corresponding author.
E-mail address: hurun@hust.edu.cn (R. Hu).
[1] These authors contributed equally to this work.

https://doi.org/10.1016/j.optlastec.2022.108689
Received 27 July 2022; Received in revised form 27 August 2022; Accepted 10 September 2022

including phosphor in glass (PiG) [15–21], ceramic phosphor [22–26] and single-crystal phosphor [27–29], which possess remarkably high thermal conductivity and stability compared with the phosphor colloid materials. Nevertheless, suffering from the complex synthesis process and high cost, these technologies have yet to be adopted on a large scale. There are also researchers trying to use external heat dissipation devices, such as heat pipes [30], thermoelectric cooling units [31], and micro-channel coolers [32–34] to cool the phosphor layer. By means of these cooling measures, the thermal issue of phosphor layer can be alleviated to some extent, but the heat of local hot spots inside the phosphor layer cannot be dissipated effectively, and the addition of external cooling devices will complicate the whole system. More recently, hexagonal boron nitride (hBN), also known as white graphene, has been reported to act as the thermally conductive filler of phosphor layer under the premise of little influence on the optical performance [35–38]. However, by simply incorporating the hBN into the phosphor colloid, the enhancement of heat transfer is very limited, since the phosphor particles are discontinuously dispersed in the polymer matrix with extremely low thermal conductivity (~0.18 W m^{-1} K^{-1}) [39]. To date, there is still a lack of simple, feasible and effective strategy to enhance the heat transfer in the phosphor layer.

Herein, we propose a promising approach to reinforce the heat transfer in phosphor layer by forming three-dimensional hBN networks in the phosphor composites. The formation mechanism of 3D network structure can be attributed to the decomposition of NH_4HCO_3, serving as sacrificial templates, and the resulting voids are filled by silicone gel to obtain the 3D/hBN-luminescent composites. Due to the existence of 3D/hBN network structure, high thermal-conductive pathways are established, thus enabling the heat generated by phosphor particles to be quickly dissipated. Moreover, the light energy can smoothly emit through the transparent silicone-filled voids, which guarantees the optical performance. The proposed 3D/hBN-luminescent composites are demonstrated to possess an excellent thermal conductivity of 0.865 W m^{-1} K^{-1}, approximately 2.2 times and 4.6 times higher than that of the randomly-distributed hBN (R/hBN) luminescent composites and traditional luminescent composites, respectively. Accordingly, the maximum working temperature of 3D/hBN-WLDs is sharply decreased by 58.4 °C and 95.2 °C compared with that of R/hBN-WLDs and traditional WLDs under the driven current of 900 mA, without deteriorating the optical performance.

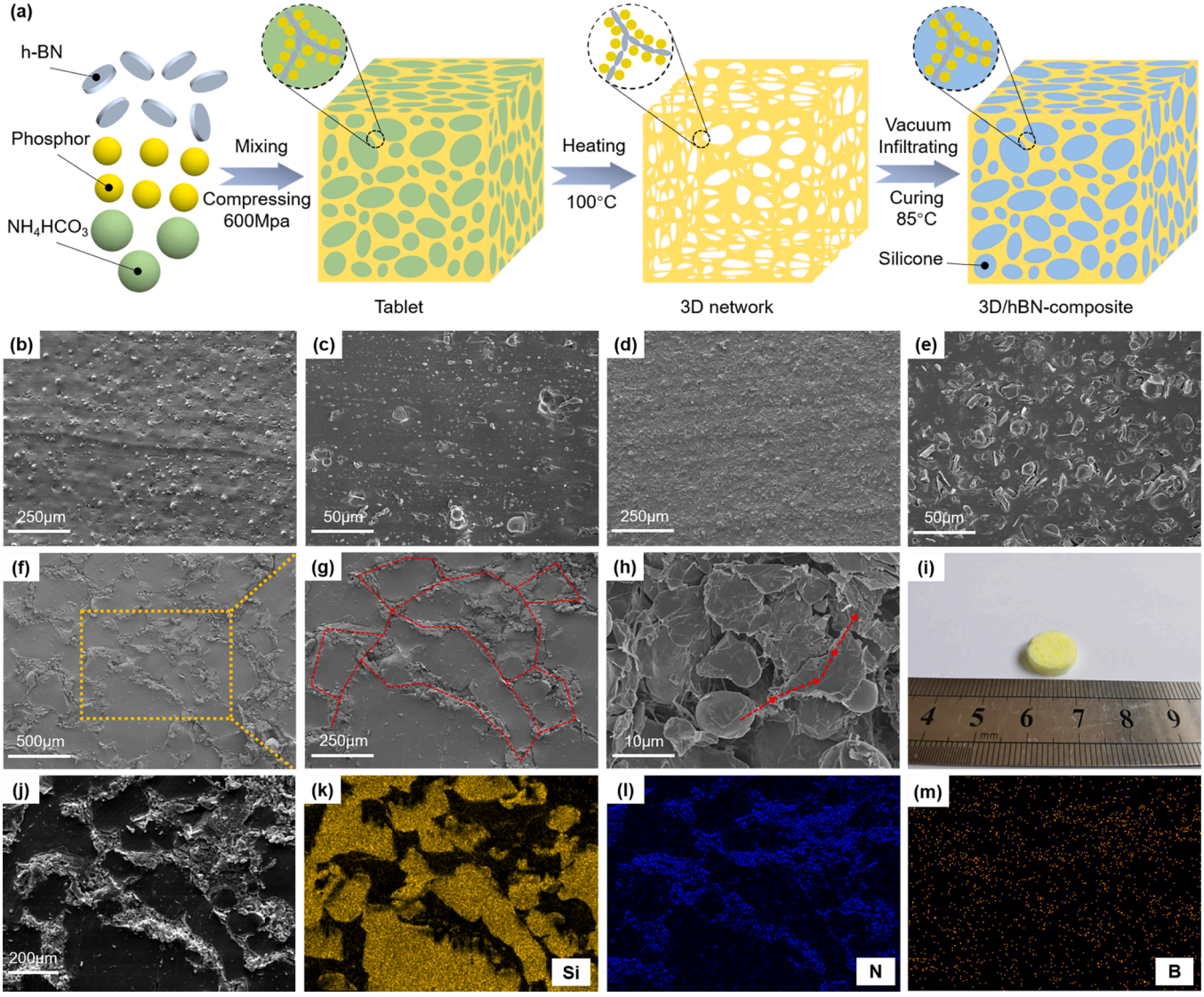

Fig. 1. (a) Schematic of the preparation process of the 3D/hBN-luminescent composites. (b)-(c) SEM images of the traditional luminescent composites under different magnifications. (d)-(e) SEM images of the R/hBN-luminescent composites under different magnifications. (f)-(h) SEM images of the 3D/hBN-luminescent composites under different magnifications. (i) Photograph of the 3D/hBN-luminescent composites. (j)-(m) SEM image and the corresponding EDS mapping images of the 3D/hBN-luminescent composites.

2. Materials and methods

2.1. Materials

Ammonium hydrogen bicarbonate (NH_4HCO_3) was purchased from Sinopharm Chemical Reagent Co., Ltd. Yellow cerium-doped yttrium aluminum garnet (YAG:Ce) phosphor with a peak wavelength of 538 nm was provided by Intematix lighting Co., Ltd. Hexagonal boron nitride (hBN) platelets with a mean size of 12 μm were obtained from Momentive. Two-component silicone was purchased from Dow Corning (SYLGARD 184, A:B = 10:1).

2.2. Preparation of the 3D/hBN-luminescent composites

The preparation process of 3D/hBN-luminescent composites is illustrated in Fig. 1a. Specifically, 0.9 g NH_4HCO_3, 0.3 g YAG phosphor, and 0.1 g hBN powders were completely mixed using a vortex mixer (VORTEX-6, Kylin-Bell, China). Then, the powder mixture was put into the tableting mold, followed by a pressure of 600 Mpa for 20 min. The obtained mixture tablet was heated in a muffle oven (XMTA-8000, Junhong, China) at 100 °C for 3 h. During the heating process, NH_4HCO_3 decomposed into ammonia, water vapor, and carbon dioxide, thus the remaining part was a three-dimensional skeleton network structure composed of hBN platelets and YAG phosphors. Next, the silicone and curing agent were evenly mixed with a weight ratio of 10:1. The obtained silicone gel was infiltrated into the as-prepared 3D/hBN skeleton networks, followed by a vacuum treatment to make the silicone gel sufficiently fill up the voids of the skeleton and remove the bubbles. Finally, the composites were cured by heating at 85 °C for 1 h to obtain the 3D/hBN-luminescent composites. For comparison, the luminescent composites with randomly-distributed hBN platelets and without hBN platelets, namely the R/hBN-luminescent composites and traditional luminescent composites were also prepared. In detail, for the preparation of R/hBN-luminescent composites, YAG phosphor, hBN powders, and silicone gel with the same mass fraction (YAG: 30 wt%; hBN: 10 wt %; silicone gel: 60 wt%) were directly mixed and then cured by vacuum heating. For the preparation of traditional luminescent composites, the process is roughly the same with that of R/hBN-luminescent composites, except for the addition of hBN platelets.

2.3. Characterizations

The scanning electron microscope (SEM) images and energy dispersive spectroscopy (EDS) mapping images of the proposed luminescent composites were observed by a field-emission SEM (Nova NanoSEM 450, FEI) operated at 15 kV. The thermal conductivity κ of the luminescent composites was calculated according to the relationship $\kappa = \alpha\rho C_p$. To be specific, the thermal diffusivity α was measured by laser flash method (LFA 457, Netzsch), where the test samples were tailored into disks with a diameter of 12.7 mm, and thin graphite films were coated on their surfaces to increase the energy absorption and the surface emittance. The density ρ was measured by an electron density meter (XF-220SD, LICHEN, China). The specific heat capacity C_p was tested by a differential scanning calorimetry (Diamond DSC, Perkin Elmer). The optical performance was measured by an integrating sphere system (ATA-1000, Everfine, China). The surface temperature of WLDs was obtained by a thermal infrared imager (SC620, FLIR) and the surface emissivity was calibrated by thermocouple before the measurements. All of the optical photographs were taken by a digital camera (Mate 30, Huawei).

3. Results and discussion

Fig. 1b and 1c show the cross-sectional morphology of the traditional luminescent composites under different magnifications. It is seen that there are only phosphor particles dispersed in the silicone matrix. Fig. 1d and 1e display the cross-sectional morphology of the R/hBN-luminescent composites under different magnifications, from which we can observe that in addition to phosphor particles, the hBN platelets are randomly distributed in the silicone matrix. The cross-sectional microstructure of 3D/hBN-luminescent composites is shown in Fig. 1f. It can be observed that owing to the decomposition of NH_4HCO_3, three-dimensional skeleton networks are formed in the luminescent composites, with silicone gel filled in the voids between the skeletons. When the heat generated by phosphor particles transferred to the skeletons, it can be rapidly dissipated through these high thermal-conductive boron nitride networks, as illustrated in Fig. 1g and 1 h. Moreover, the transparent silicone gel in the holes of 3D skeleton networks provides propagating paths for the light energy, thus ensuring the optical performance. Fig. 1i displays the photograph of the proposed 3D/hBN-luminescent composites. It is worth mentioning that the shape and size of the luminescent composites can be easily adjusted by designing the tableting molds, which indicates the potential for large-scale manufacturing. In order to verify the composition of the 3D skeleton network structure, the energy dispersive spectroscopy (EDS) was used to analyze the element distribution. For a network structure shown in Fig. 1j, the distributions of silicon (Si), nitrogen (N), and boron (B) are illustrated in Fig. 2k, 2 l, and 2 m, respectively. It can be confirmed from EDS mapping images that the skeleton network structure is indeed composed of born nitride and the voids of the networks are filled with silicone gel.

The measured thermal conductivity of traditional luminescent composites (T-composites), randomly-distributed hBN luminescent composites (R/hBN-composites), and three-dimensional hBN luminescent composites (3D/hBN-composites) is illustrated in Fig. 2a , and the detailed calculation parameters are listed in the Supplementary Material (Table S1-S3). It is observed that the T-composites exhibit extremely low thermal conductivity, which is approximately 0.18 W m^{-1} K^{-1} in the ambient temperature range of 25 °C to 125 °C. The reason for the poor thermal conductivity is generally ascribed to the disordered molecular chains and weak molecular interactions in the silicone matrix. To be specific, the heat carriers in polymer are phonons, while the mean free path of heat-conducting phonons is greatly reduced due to the random orientation of molecular chains and weak molecular interactions [40]. Moreover, strong phonon scattering will occur in the amorphous regions of the silicone matrix, thus hindering the phonon transport [41]. When a quantity of boron nitride platelets is randomly mixed into the traditional luminescent composites, namely the R/hBN-composites, a slight enhancement of thermal conductivity can be observed, approximately a two-fold increase. This can be explained that high thermal-conductive hBN platelets play the role of thermal enhancement fillers, but the randomly-distributed hBN platelets are still discontinuously dispersed in the silicone matrix with extremely low thermal conductivity, thus limiting the performance improvement. However, with the same mass fraction, the 3D/hBN-composites are demonstrated to possess an excellent thermal conductivity of 0.865 W m^{-1} K^{-1} at 25 °C, which is about 2.2 times and 4.6 times higher than that of the R/hBN-composites and the T-composites, respectively. The significant reinforcement of thermal conductivity can be attributed to the existence of interconnected 3D skeleton networks, which provide pathways for phonon transport, thus promoting the heat generated by phosphor particles being efficiently conducted out. Note that with the increase of ambient temperature, the thermal conductivity of composites will experience a slight decrease. This can be explained by the fact that atoms in the lattice vibrate more violently at higher temperature, leading to stronger phonon scattering [42].

To further explore the underlying mechanism for the thermal conductivity enhancement of these composites, a two-dimensional finite element simulation was carried out, and the details about the physical models and boundary conditions are presented in the Fig. S1. Fig. 2b-2d display the simulated temperature distributions of the three kinds of composites, where cycles represent phosphor particles, rectangles

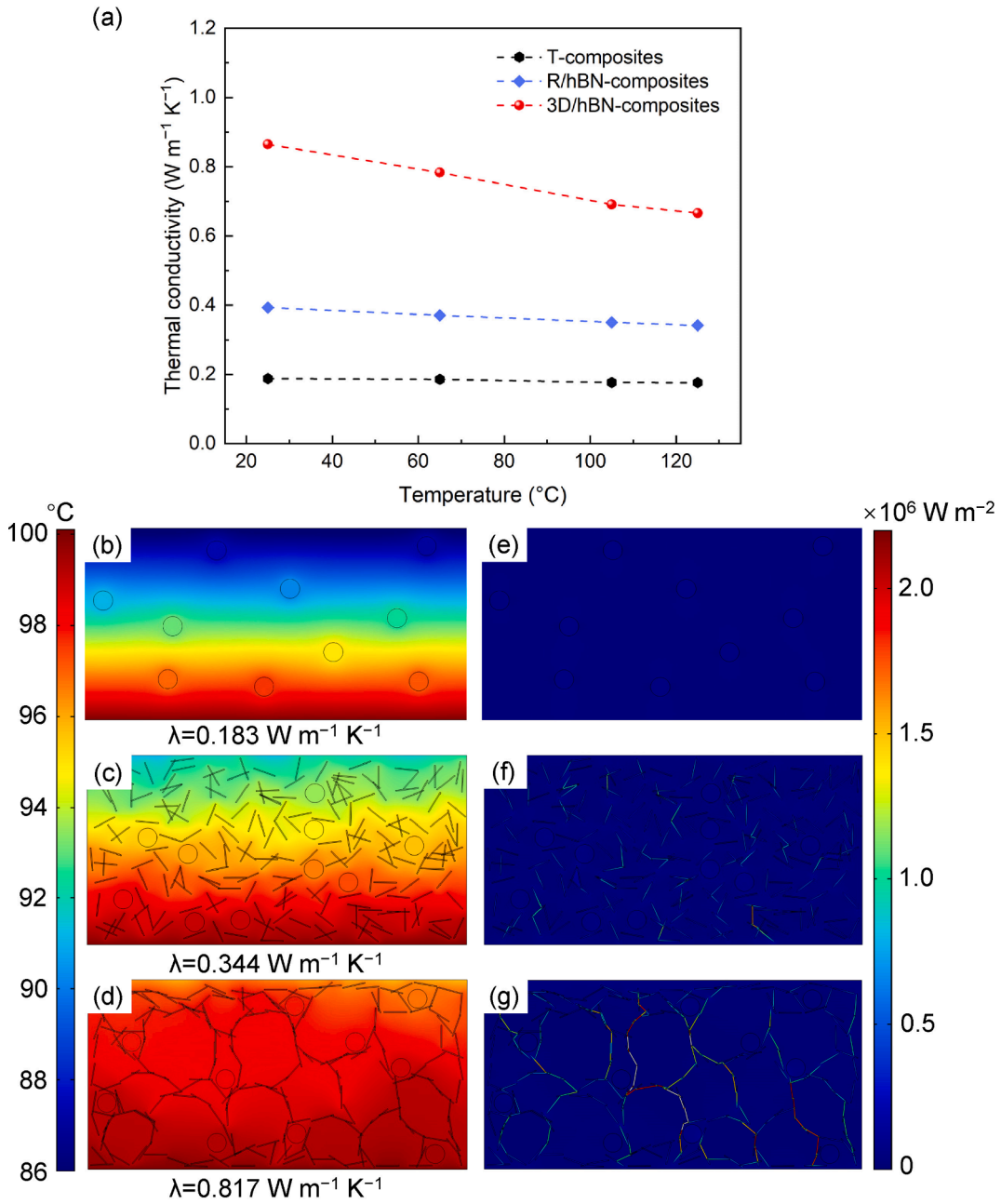

Fig. 2. (a) Measured thermal conductivity of T-composites, R/hBN-composites, and 3D/hBN-composites under different ambient temperature. Simulated temperature distributions of (b) T-composites, (c) R/hBN-composites, and (d) 3D/hBN-composites. Simulated heat flux distributions of (e) T-composites, (f) R/hBN-composites, and (g) 3D/hBN-composites.

represent hBN platelets, and other regions represent silicone gel. It can be observed that under the same bottom-side temperature, the top-side temperature of 3D/hBN-composites is obviously the highest among the three composites, namely the temperature difference is the smallest, indicating the heat transfer in the 3D/hBN-composites is the most efficient. Furthermore, from the simulated heat flux distributions illustrated in Fig. 2e-2 g, we can clearly find that the heat flux density in hBN is remarkably higher than that in silicone gel or phosphor particles, revealing that the heat transfer in the composites mainly depends on the hBN. In the R/hBN-composites, although the heat flux density increases with the addition of hBN when compared with that of T-composites, the improvement is limited because the silicone gel between hBN platelets also creates obstacles for the phonon transport. Unlike the other two composites, there exist continuous heat transfer channels in the 3D/hBN-composites due to the interconnected hBN platelets, which provide pathways for the heat-conducting phonons and can be considered as the key to reinforce the heat transfer performance.

In order to study the optical performance of the proposed composites, they were combined with a blue laser diode to form simple white lighting devices, where the composites were fixed on an aluminum-alloy heat sink coated with reflective coatings and positioned at specific angles to the light path of the laser diode. These luminescent devices were placed into an integrating sphere for optical performance test, as illustrated in Fig. 3a. Fig. 3b displays the spectral power distributions and their corresponding optical properties of the white lighting devices composed of T-composites (T-WLDs), R/hBN-composites (R/hBN-WLDs), and 3D/hBN-composites (3D/hBN-WLDs), respectively, under the driving current of 700 mA. It can be observed that the spectral distributions of the three luminescent devices are similar under the same driving current, including blue light peaks and the excited yellow light

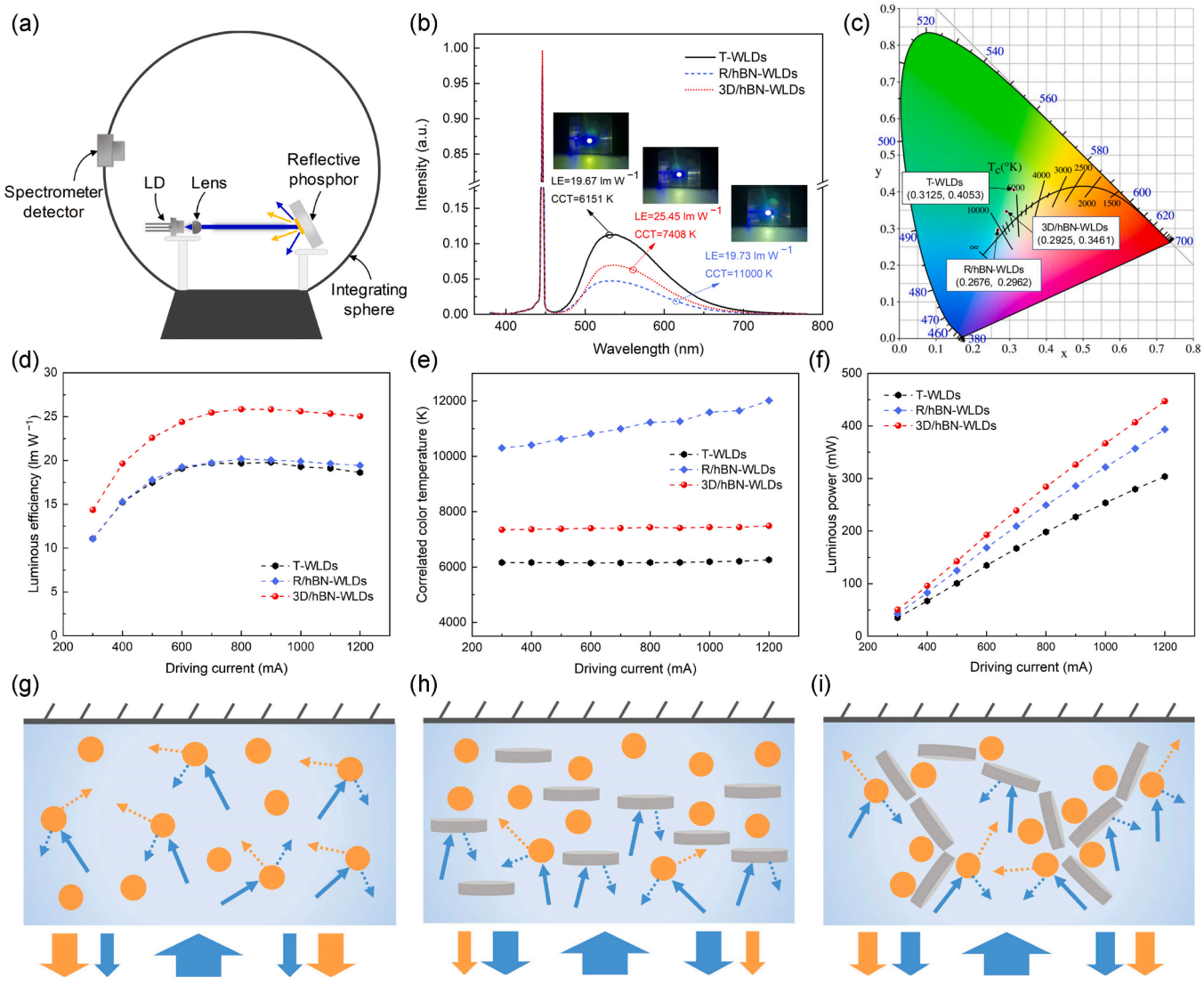

Fig. 3. (a) Schematic of optical performance test. (b) Spectral power distributions and optical properties of the three kinds of WLDs under the driving current of 700 mA. The insets show their illuminated photographs. (c) The coordinates of these WLDs in the CIE 1931 diagram under the driving current of 700 mA. (d) Luminous efficiency (LE) of these WLDs under different currents from 300 to 1200 mA. (e) Correlated color temperature (CCT) of these WLDs under different currents from 300 to 1200 mA. (f) Luminous power of these WLDs under different currents from 300 to 1200 mA. Schematic of the optical processes in (g) T-composites, (h) R/hBN-composites, and (i) 3D/hBN-composites.

spectrum, which are consistent with the principle of laser-excited white lighting. Moreover, the T-WLDs are found to possess highest yellow light intensity, indicating that the yellow light excited in the T-composites is the most among the three kinds of composites. The yellow light intensity of 3D/hBN-WLDs is slightly lower than that of T-WLDs, leading to a moderate increase in correlated color temperature (CCT) from 6151 K to 7408 K, which is still within the acceptable range considering the comprehensive performance. It is seen that the yellow light intensity of R/hBN-WLDs is the lowest, corresponding to the highest CCT among these WLDs. The insets in Fig. 3b display the actual illuminated photographs of the three devices, which are in good agreement with the spectral measurement results. The coordinates of these WLDs in the CIE 1931 diagram under the driving current of 700 mA are illustrated in Fig. 3c, from which we can observe that the location of 3D/hBN-WLDs is close to the central region of Planck blackbody curve, and is between the coordinates of T-WLDs and R/hBN-WLDs. Fig. 3d-3f provide the luminous efficiency (LE), the correlated color temperature (CCT), and the luminous power of these WLDs under different currents from 300 to 1200 mA. The results suggest that with the increase of driving current, the LE of these WLDs exhibits the trend of increasing in the early stage and slightly decreasing later. This is mainly determined by the characteristics of laser diodes, specifically, their electro-optical conversion efficiency will increase with the increase of the driving current, but when the current is too large, the rise of temperature will lead to a slight decrease in their efficiency, further resulting in the decrease of LE. In addition, it is noted that the LE of 3D/hBN-WLDs is found to be higher than that of T-WLDs or R/hBN-WLDs. This can be explained by the fact that the 3D/hBN-composites absorb the least blue laser light and have the highest light conversion ratio (the ratio of converted yellow light to absorbed blue laser light) among the three composites, which are illustrated in Fig. S2a-2b. From Fig. 3e, we can observe that the CCT of 3D/hBN-WLDs and T-WLDs remains stable with the increase of driving current, and the CCT of R/hBN-WLDs is found to be the highest among the three composites. Fig. 3f shows the luminous power of these composites. It is seen that under different driving currents, the luminous power of 3D/hBN-WLDs is the largest, while that of T-WLDs remains the smallest. To better understand the reasons for the above optical performance, the optical processes in the three composites are described in

Fig. 3g-3i, where yellow circles represent phosphor particles, gray rectangles represent hBN platelets, and blue regions represent silicone gel. Concretely, for T-composites, there are only phosphor particles and silicone gel in the composites, enabling a longer optical path as well as a deeper penetration depth of the incident blue light. Thus, the blue light can excite more phosphor particles to emit yellow light during the propagation in the luminescent layer, resulting in lower CCT. Meanwhile, the loss caused by photoluminescence will also increase, which will lead to the reduction of luminous power. For R/hBN-composites where hBN platelets are added, the deposition effect during the preparation process makes the hBN platelets tend to be aligned in parallel. The horizontally dispersed hBN platelets will scatter the incident blue light, resulting in a shortened penetration depth of blue light and consequently a decrease of excited yellow light, which in turn increases the CCT. Accordingly, the photoluminescence loss will decrease, thus obtaining higher luminous power. Compared with 3D network structure, this parallel structure will greatly reduce the optical path of the incident blue light, in which case the excited yellow light will be reduced and the CCT will consequently increase. Moreover, the densely aligned hBN platelets will increase the scattering of the incident blue light, leading to the loss of luminous power, and thus the R/hBN-WLDs exhibit lower luminous power than that of 3D/hBN-WLDs. Since the LE is determined by both luminous power and spectral intensity, the 3D/hBN-WLDs possess the highest LE, followed by R/hBN-WLDs and T-WLDs. The above results have demonstrated that the 3D network structure dose not deteriorate the optical performance of 3D/hBN-composites when compared with that of T-composites.

To investigate the thermal performance of these WLDs, we first measured and calculated the heat power in the three kinds of luminescent composites under different driving currents according to the law of energy conservation, as shown in Fig. 4a. The obtained results reveal that the heat generation increases with the increase of driving current, and the luminescent composites of T-WLDs generate the most heat among three composites, while the heat generated in the 3D/hBN-WLDs is the least. Based on the calculated heat power, the steady-state temperature fields of three luminescent devices were simulated by finite element method. Fig. 4b illustrates the physical model of the simulations, and the details about the simulation process are presented in the Supplementary Material. From the simulated temperature distributions shown in Fig. 4c-4d, it can be observed that under the driving current of 700 mA, there occurs obvious heat accumulation in the laser irradiation area of T-WLDs, leading to localized high temperature of 117.6 °C in the luminescent composites. When randomly-distributed hBN is added, namely the R/hBN-WLDs, the maximum temperature is reduced to 73.5 °C. However, with the same mass fraction of hBN, the temperature of 3D/hBN-WLDs containing interconnected network structure is

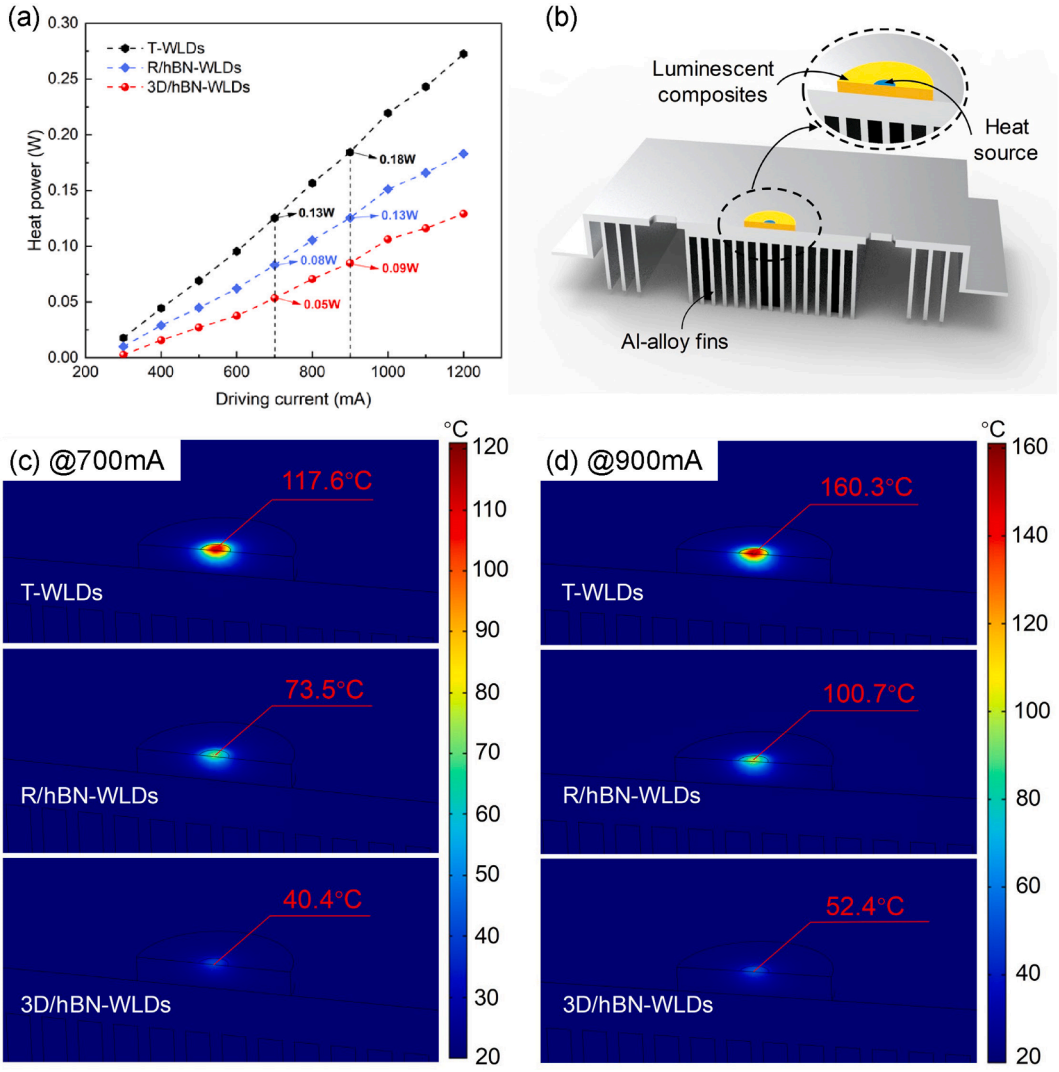

Fig. 4. (a) Measured heat power in T-WLDs, R/hBN-WLDs, and 3D/hBN-WLDs under different driving currents from 300 to 1200 mA. (b) Physical model for the thermal simulation. Simulated temperature distributions of the three WLDs under driving currents of (c) 700 mA and (d) 900 mA, respectively.

dramatically decreased to 40.4 °C, which is 77.2 °C and 33.1 °C lower than that of T-WLDs and R/hBN-WLDs, respectively. Moreover, it is worth mentioning that the thermal performance of 3D/hBN-WLDs is more significant at higher driving current. Concretely, when the driving current is increased to 900 mA, the maximum temperature of 3D/hBN-WLDs remains low value of 52.4 °C, but the temperature of T-WLDs and R/hBN-WLDs increased to 160.3 °C and 100.7 °C, which are 107.9 °C and 48.3 °C higher than that of 3D/hBN-WLDs. Consequently, it is demonstrated from the above results that the 3D-hBN network structure can effectively reduce the working temperature of luminescent devices.

To validate the accuracy of the simulation results, the surface temperature distributions of these WLDs under 700 mA and 900 mA were measured by a thermal infrared imager, as illustrated in Fig. 5a-5b. The surface emissivity of the test samples was set as 0.96, and the distance between the camera lens and the samples was set to 0.3 m, as shown in Fig. 5c. Note that all test results were recorded after the temperature had reached stability, and the values given in the figures are the highest temperature in the spot regions. It can be seen from these infrared images that the actual working temperature is in good agreement with the results obtained by finite element simulation, and the maximum relative deviation between the experiment and simulation is 14.1%, which is within the permissible range of error. Moreover, the experimental results also demonstrate the excellent thermal performance of the 3D/hBN-WLDs. To be specific, when 3D/hBN-composites were utilized to replace T-composites, a significant temperature reduction of 68.1 °C can be observed under the driving current of 700 mA. And when the driving current increases to 900 mA, the cooling effect reaches 95.2 °C. Furthermore, the variation of maximum surface temperature under different driving currents from 300 to 1200 mA of these WLDs were measured and illustrated in Fig. 5d. The results reveal that with the increase of driving current, the maximum surface temperature of the three devices exhibits approximately linear increase trend, among which the temperature rise of 3D/hBN-WLDs is the slowest. Besides, the excellent thermal performance of 3D/hBN-WLDs is more distinct under higher driving current. It is noted that a sudden jump in temperature can be observed when the driving current increases to 1200 mA, indicating that the thermal quenching effect occurs at this moment. A more serious consequence is that continuous working under this current will further aggravate the thermal quenching phenomenon, and even lead to carbonization of silicone gel, as shown in the inset of Fig. 5d. The above

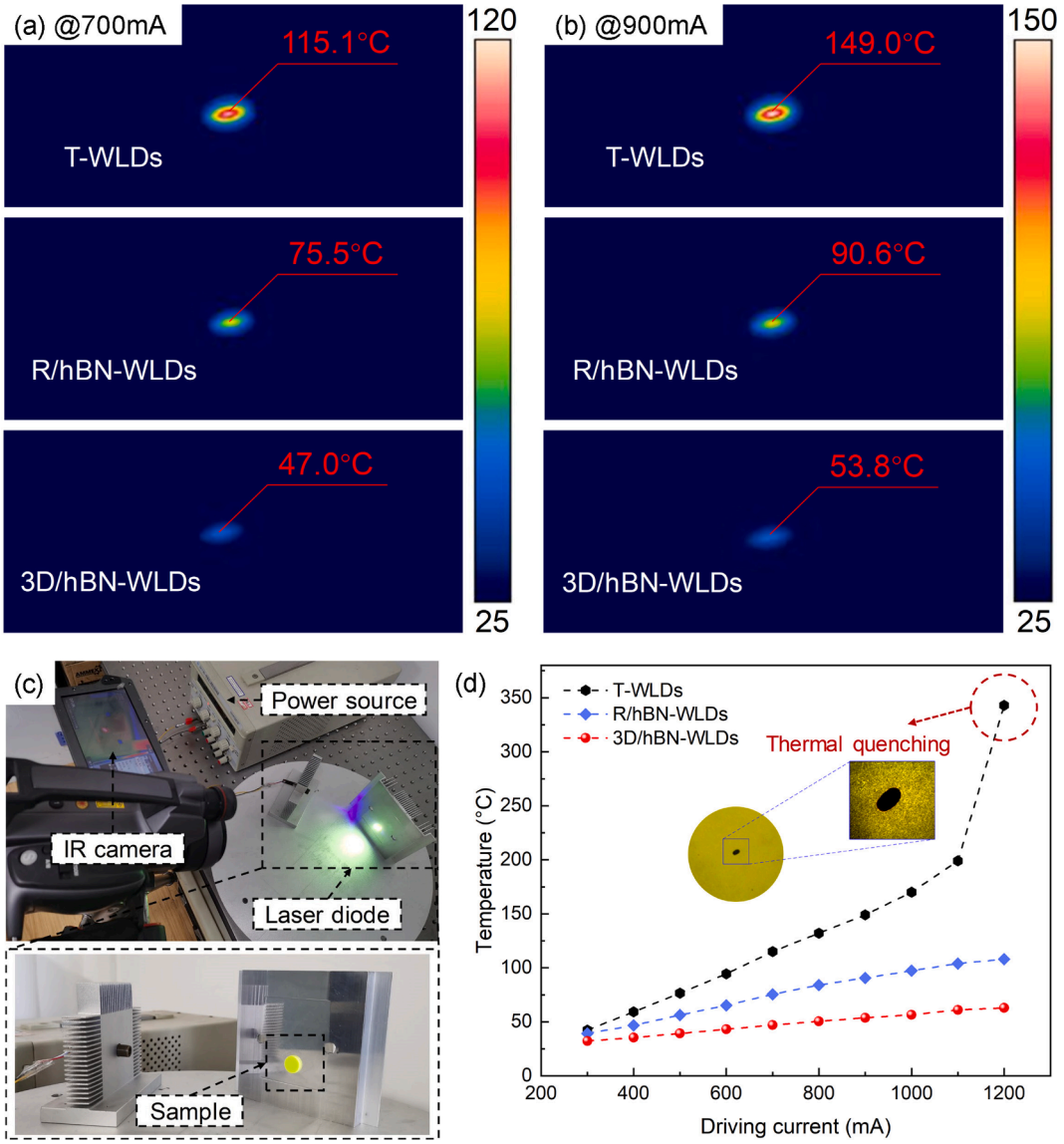

Fig. 5. Measured surface temperature distributions of the three WLDs under driving currents of (a) 700 mA and (b) 900 mA, respectively. (c) Temperature measurement setup. (d) Measured maximum surface temperature of these WLDs under different driving currents from 300 to 1200 mA. The inset shows the thermal quenching phenomenon of the luminescent composites.

results have proven the critical role of thermal management of the luminescent composites, which is key to achieve high-power laser-excited white lighting.

4. Conclusions

To summarize, we demonstrated an effective cooling approach to enhance the heat transfer in phosphor layer by establishing 3D-hBN networks inside the luminescent composites. Benefited from the hBN network structure, the proposed 3D/hBN-composites possess remarkably high thermal conductivity of 0.865 W m^{-1} K^{-1}, approximately 2.2 times and 4.6 times higher than that of the R/hBN-composites and T-composites, respectively. When applied to laser-excited white lighting devices, the maximum working temperature of 3D/hBN-WLDs is dramatically decreased by 58.4 °C and 95.2 °C compared with that of R/hBN-WLDs and T-WLDs under the driving current of 900 mA, without deteriorating the optical performance. This work opens up a new opportunity to solve the thermal issue in the phosphor layer, which is expected to promote further applications of laser-excited white lighting in high-power and high-brightness scenarios, and beyond.

CRediT authorship contribution statement

Weixian Zhao: Conceptualization, Methodology, Investigation, Writing – original draft. **Bin Xie:** Conceptualization, Methodology, Investigation, Writing – original draft. **Yang Peng:** Data curation, Methodology. **Song Xue:** Validation. **Xiaobing Luo:** Supervision, Writing – review & editing. **Run Hu:** Conceptualization, Supervision, Writing – review & editing, Funding acquisition.

Declaration of Competing Interest

The authors declare that they have no known competing financial interests or personal relationships that could have appeared to influence the work reported in this paper.

Data availability

Data will be made available on request.

Acknowledgements

The authors acknowledge the financial support from the National Natural Science Foundation of China (52106089, 52076087, 52161160332), China Postdoctoral Science Foundation (2021M691120), the Open Project Program of Wuhan National Laboratory for Optoelectronics (No. 2021WNLOKF004), and Postdoctoral Creative Research Funding of Hubei Province.

Appendix A. Supplementary material

Supplementary data to this article can be found online at https://doi.org/10.1016/j.optlastec.2022.108689.

References

[1] X. Luo, R. Hu, S. Liu, K. Wang, Heat and fluid flow in high-power LED packaging and applications, Prog. Energ. Combust. 56 (2016) 1–32.
[2] P. Pust, P.J. Schmidt, W. Schnick, A revolution in lighting, Nat. Mater. 14 (2015) 454–458.
[3] E.F. Schubert, J.K. Kim, H. Luo, J.Q. Xi, Solid-state lighting—a benevolent technology, Rep. Prog. Phys. 69 (2006) 3069–3099.
[4] E. Kioupakis, P. Rinke, K.T. Delaney, C.G. Van de Walle, Indirect Auger recombination as a cause of efficiency droop in nitride light-emitting diodes, Appl. Phys. Lett. 98 (2011), 161107.
[5] M. Auf der Maur, A. Pecchia, G. Penazzi, W. Rodrigues, A. Di Carlo, Efficiency drop in green InGaN/GaN light emitting diodes: the role of random alloy fluctuations, Phys. Rev. Lett. 116 (2016), 027401.
[6] S. Li, L. Wang, N. Hirosaki, R.J. Xie, Color conversion materials for high-brightness laser-driven solid-state lighting, Laser Photonics Rev. 12 (2018) 1800173.
[7] J.J. Wierer, J.Y. Tsao, D.S. Sizov, Comparison between blue lasers and light-emitting diodes for future solid-state lighting, Laser Photonics Rev. 7 (2013) 963–993.
[8] B. Xie, R. Hu, X. Luo, Manipulating heat transport of photoluminescent composites in LEDs/LDs, J. Appl. Phys. 130 (2021), 070906.
[9] Y. Ma, X. Luo, Packaging for laser-based white lighting: status and perspectives, J. Electron. Packaging 142 (2020), 010801.
[10] Y. Ma, X. Luo, Enhancing opto-thermal performances of the reflective phosphor-converted laser diode by stacking a sapphire substrate for double-sided phosphor cooling, Int. J. Heat Mass Tran. 143 (2019), 118600.
[11] X. Luo, X. Fu, F. Chen, H. Zheng, Phosphor self-heating in phosphor converted light emitting diode packaging, Int. J. Heat Mass Tran. 58 (2013) 276–281.
[12] X. Luo, R. Hu, Calculation of the phosphor heat generation in phosphor-converted light-emitting diodes, Int. J. Heat Mass Tran. 75 (2014) 213–217.
[13] V. Bachmann, C. Ronda, A. Meijerink, Temperature quenching of yellow Ce^{3+} luminescence in YAG:Ce, Chem. Mater. 21 (2009) 2077–2084.
[14] Y.H. Kim, P. Arunkumar, B.Y. Kim, S. Unithrattil, E. Kim, S.H. Moon, J.Y. Hyun, K. H. Kim, D. Lee, J.S. Lee, W.B. Im, A zero-thermal-quenching phosphor, Nat. Mater. 16 (2017) 543–550.
[15] Q.-Q. Zhu, X.-J. Wang, L. Wang, N. Hirosaki, T. Nishimura, Z.-F. Tian, Q. Li, Y.-Z. Xu, X. Xu, R.-J. Xie, β-Sialon: Eu phosphor-in-glass: a robust green color converter for high power blue laser lighting, J. Mater. Chem. C 3 (2015) 10761–10766.
[16] P. Zheng, S. Li, L. Wang, T.L. Zhou, S. You, T. Takeda, N. Hirosaki, R.J. Xie, Unique color converter architecture enabling phosphor-in-glass (PiG) films suitable for high-power and high-luminance laser-driven white lighting, ACS Appl. Mater. Inter. 10 (2018) 14930–14940.
[17] X. Zhang, J. Yu, J. Wang, B. Lei, Y. Liu, Y. Cho, R.-J. Xie, H.-W. Zhang, Y. Li, Z. Tian, Y. Li, Q. Su, All-inorganic light convertor based on phosphor-in-glass engineering for next-generation modular high-brightness white LEDs/LDs, ACS Photonics 4 (2017) 986–995.
[18] Z. Zheng, Y. Luo, H. Yang, Z. Yi, J. Zhang, Q. Song, W. Yang, C. Liu, X. Wu, P. Wu, Thermal tuning of terahertz metamaterial properties based on phase change material vanadium dioxide, Phys. Chem. Chem. Phys. 24 (2022) 8846–8853.
[19] H. Yang, Y. Zhang, Y. Zhang, Y. Zhao, X. Liang, G. Chen, Y. Liu, W. Xiang, Designed glass frames full color in white light-emitting diodes and laser diodes lighting, Chem. Eng. J. 414 (2021), 128754.
[20] F, Zhao, J, Lin, Z, Lei, Z, Yi, F, Qin, J, Zhang, L, liu, X, Wu, W, Yang, P, Wu, Realization of 18.97% theoretical efficiency of 0.9μm thick c-Si/ZnO heterojunction ultrathin-film solar cells via surface plasmon resonance enhancement, Phys. Chem. Chem. Phys., 24 (2022) 4871-4880.
[21] Y. Peng, Y. Mou, Q. Sun, H. Cheng, M. Chen, X. Luo, Facile fabrication of heat-conducting phosphor-in-glass with dual-sapphire plates for laser-driven white lighting, J. Alloy. Compd. 790 (2019) 744–749.
[22] S. Li, Q. Zhu, L. Wang, D. Tang, Y. Cho, X. Liu, N. Hirosaki, T. Nishimura, T. Sekiguchi, Z. Huang, R.-J. Xie, $CaAlSiN_3$:Eu^{2+} translucent ceramic: a promising robust and efficient red color converter for solid state laser displays and lighting, J. Mater. Chem. C 4 (2016) 8197–8205.
[23] M. Xu, J. Chang, J. Wang, C. Wu, F. Hu, Al_2O_3-YAG: Ce composite ceramics for high-brightness lighting, Opt. Express 27 (2019) 872–885.
[24] S. Li, Q. Zhu, D. Tang, X. Liu, G. Ouyang, L. Cao, N. Hirosaki, T. Nishimura, Z. Huang, R.-J. Xie, Al_2O_3–YAG: Ce composite phosphor ceramic: a thermally robust and efficient color converter for solid state laser lighting, J. Mater. Chem. C 4 (2016) 8648–8654.
[25] D.Y. Kosyanov, X. Liu, A.A. Vornovskikh, A.P. Zavjalov, A.M. Zakharenko, A. A. Kosianova, A.N. Fedorets, O.O. Shichalin, A.A. Leonov, W. Li, J. Li, Al_2O_3–Ce: YAG composite ceramics for high brightness lighting: cerium doping effect, J. Alloy. Compd. 887 (2021), 161486.
[26] Z. Zheng, Y. Zheng, Y. Luo, Z. Yi, J. Zhang, Z. Liu, W. Yang, Y. Yu, X. Wu, P. Wu, Switchable terahertz device combining ultra-wideband absorption and ultra-wideband complete reflection, Phys. Chem. Chem. Phys. 24 (2022) 2527–2533.
[27] T.W. Kang, K.W. Park, J.H. Ryu, S.G. Lim, Y.M. Yu, J.S. Kim, Strong thermal stability of $Lu_3Al_5O_{12}$:Ce^{3+} single crystal phosphor for laser lighting, J. Lumin. 191 (2017) 35–39.
[28] M. Cantore, N. Pfaff, R.M. Farrell, J.S. Speck, S. Nakamura, S.P. DenBaars, High luminous flux from single crystal phosphor-converted laser-based white lighting system, Opt. Express 24 (2016) A215–A221.
[29] S. Arjoca, E.G. Víllora, D. Inomata, K. Aoki, Y. Sugahara, K. Shimamura, Ce: $(Y_{1-x}Lu_x)_3Al_5O_{12}$ single-crystal phosphor plates for high-brightness white LEDs/LDs with high-color rendering (Ra > 90) and temperature stability, Mater. Res. Express 1 (2014), 025041.
[30] X. Ding, M. Li, Z. Li, Y. Tang, Y. Xie, X. Tang, T. Fu, Thermal and optical investigations of a laser-driven phosphor converter coated on a heat pipe, Appl. Therm. Eng. 148 (2019) 1099–1106.
[31] J. Park, J. Kim, H. Kwon, Phosphor-aluminum composite for energy recycling with high-power white lighting, Adv. Opt. Mater. 5 (2017) 1700347.
[32] A. Kozłowska, P. Łapka, M. Seredyński, M. Teodorczyk, E. Dąbrowska-Tumańska, Experimental study and numerical modeling of micro-channel cooler with micro-pipes for high-power diode laser arrays, Appl. Therm. Eng. 91 (2015) 279–287.
[33] M. Datta, H.-W. Choi, Microheat exchanger for cooling high power laser diodes, Appl. Therm. Eng. 90 (2015) 266–273.
[34] S. Baraty Beni, A. Bahrami, M.R. Salimpour, Design of novel geometries for microchannel heat sinks used for cooling diode lasers, Int. J. Heat Mass Tran. 112 (2017) 689–698.

[35] S. Zhou, Y. Ma, X. Zhang, W. Lan, X. Yu, B. Xie, K. Wang, X. Luo, White-light-emitting diodes from directional heat-conducting hexagonal boron nitride quantum dots, ACS Appl. Nano Mater. 3 (2019) 814–819.
[36] B. Xie, H. Liu, R. Hu, C. Wang, J. Hao, K. Wang, X. Luo, Targeting cooling for quantum dots in white QDs-LEDs by hexagonal boron nitride platelets with electrostatic bonding, Adv. Funct. Mater. 28 (2018) 1801407.
[37] B. Xie, Y. Wang, H. Liu, J. Ma, S. Zhou, X. Yu, W. Lan, K. Wang, R. Hu, X. Luo, Targeting cooling for quantum dots by 57.3°C with air-bubbles-assembled three-dimensional hexagonal boron nitride heat dissipation networks, Chem. Eng. J. 427 (2022), 130958.
[38] X. Yang, S. Zhou, B. Xie, X. Yu, X. Zhang, L. Xiang, K. Wang, X. Luo, Enhancing hat dssipation of qantum dots in high-power white LEDs by thermally conductive composites annular Fins, IEEE Electr. Device L. 42 (2021) 1204–1207.
[39] C. Yuan, X. Luo, A unit cell approach to compute thermal conductivity of uncured silicone/phosphor composites, Int. J. Heat Mass Tran. 56 (2013) 206–211.
[40] W. Zhao, R. Hu, Toward high-thermal-conductivity polymers, Matter 4 (2021) 3799–3801.
[41] V. Singh, T.L. Bougher, A. Weathers, Y. Cai, K. Bi, M.T. Pettes, S.A. McMenamin, W. Lv, D.P. Resler, T.R. Gattuso, D.H. Altman, K.H. Sandhage, L. Shi, A. Henry, B. A. Cola, High thermal conductivity of chain-oriented amorphous polythiophene, Nat. Nanotechnol. 9 (2014) 384–390.
[42] M. Raeisi, S. Ahmadi, A. Rajabpour, Modulated thermal conductivity of 2D hexagonal boron arsenide: a strain engineering study, Nanoscale 11 (2019) 21799–21810.